

## Supporting Information

### Spectroscopic and Mechanistic Insights into Solvent Mediated Excited-State Proton Transfer and Aggregated Induced Emission: Introduction of Methyl Group onto 2-(o-Hydroxyphenyl)benzoxazole

Yu Li<sup>§</sup>, Yuanyue Wang<sup>§</sup>, Xiaoqing Feng<sup>\*#</sup>, Yanying Zhao<sup>\*§</sup>,

<sup>§</sup> Department of Chemistry, Zhejiang Sci-Tech University, Hangzhou 310018, China

<sup>#</sup> School of Pharmacy & School of Medicine, Changzhou University, Changzhou 213164, China

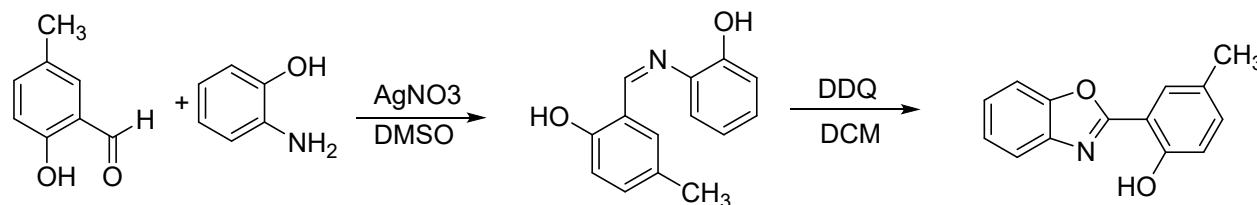
\* Corresponding author: [fxqfw@163.com](mailto:fxqfw@163.com) (Feng X.); [yyzhao@zstu.edu.cn](mailto:yyzhao@zstu.edu.cn) (Y. Zhao)

## Experimental Methods and Calculation Details

### Materials and general methods

Solvents were purchased from various commercial sources and used without further purification unless otherwise stated. Spectroscopic grade solvents were used in the UV/Vis and fluorescence spectroscopic measurements. Analytical thin-layer chromatography (TLC) was performed using pre-coated TLC plates with silica gel 60 F254 or with aluminum oxide 60 F254 neutral. Flash column chromatography was performed using silica (230-400 mesh) gel or alumina oxide (80-200 mesh) as the stationary phases. <sup>1</sup>H NMR spectra were acquired on NMR Spectrometer (Bruker, AVANCE III, 400MHz, Germany) to confirm its structure. All chemical shifts were reported in  $\delta$  units relative to tetramethylsilane. DMSO was treated with alumina gel prior to use. Electronic absorption spectra were recorded by a UV-Vis spectrophotometer (Shimadzu, 3600-Plus, Japan). Emission and excitation spectra were obtained from fluorescence spectrophotometers (HORIBA Fluoramax-4, USA and Hitachi F-7000, Japan).

### Synthesis of HBO-p-CH<sub>3</sub> Compound.



2-Hydroxy-5-methylbenzaldehyde (4.0 mmol), 2-aminophenol (4.4 mol) and catalytic dose of silver nitrate ( $\text{AgNO}_3$ ) were mixed in a 50 mL round-bottom flask with 20 mL dimethylsulfoxide (DMSO). Then, the mixture was stirred for 4 h in a water bath condition ( $35^\circ\text{C}$ ). The TLC template (PE:EA=3:1) was employed to monitor the progress of the reaction. The mixture was cooled to room temperature after the reaction was finished and then 60 mL dichloromethane (DCM) was added to the above room mixture, and then a large amount of saturated salt water was applied to extract the organic layer, which was span and dried to obtain the pure (Z)-2-(((2-hydroxyphenyl)imino)methyl)-4-methylphenol. Next, (Z)-2-(((2-hydroxyphenyl)imino)methyl)-4-methylphenol and 2,3-dichloro-5,6-difluoro-p-benzoquinone (DDQ) in a molar ratio of 1:1.1 were mixed in 60 mL dichloromethane. Similarly, the reaction was stirred at  $40^\circ\text{C}$  for 4 h and monitored by TLC (PE:EA=5:1). Finally, by filtration the filtrate was retained and spin-dried and recrystallized with methanol to obtain the target product HBO-pCH<sub>3</sub>. Figure S1 showed the  $^1\text{H}$  NMR of HBO-pCH<sub>3</sub> in DMSO-d<sub>6</sub> (11.03(s,1H), 7.87(dt, J = 9.4, 3.1 Hz, 3H), 7.50 (m, 2H), 7.36 (dd, J = 8.4, 2.3 Hz, 1H), 7.06(d, J = 8.4 Hz, 1H), 2.36 (s, 3H).

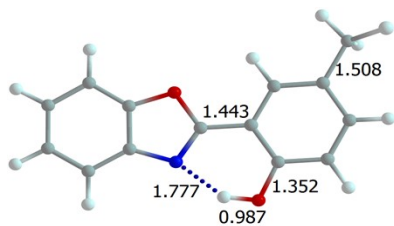
## Calculation

All the calculations are performed using the Gaussian 09W program suite<sup>S1</sup>. The geometries were optimized by DFT and TDDFT in the ground state and excited state, respectively, using the basis set 6-311+G(d,p) with Becke's three-parameter exchange functional accompanying the Lee-Yang-Parr nonlocal correlation functional (B3LYP)<sup>S2-S3</sup> and the solvent effects with the polarizable continuum model (PCM)<sup>S4</sup>. In addition, to avoid the misrepresentation of weak interactions, density functional theory including dispersion correction (DFT-D3)<sup>S5-S6</sup> was considered.

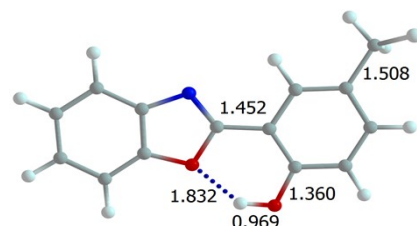
## References

- S1. Frisch M. J.; Trucks G. W.; Schlegel H. B.; Scuseria G. E.; Robb M. A.; Cheeseman J. R.; Scalmani G.; Barone V.; Mennucci B.; Petersson G. A.; Nakatsuji H.; Caricato M.; Li X.; Hratchian H. P.; Izmaylov A. F.; Bloino J.; Zheng G.; Sonnenberg J. L.; Hada M.; Ehara M.; Toyota K.; Fukuda R.; Hasegawa J.; Ishida M.; Nakajima T.; Honda Y.; Kitao O.; Nakai H.; Vreven T.; Montgomery J. J. A.; Peralta J. E.; Ogliaro F.; Bearpark M.; Heyd J. J.; Brothers E.; Kudin, K. N.; Staroverov V. N.; Kobayashi R.; Normand J.; Raghavachari K.; Rendell A.; Burant J. C.; Iyengar S. S.; Tomasi J.; Cossi M.; Rega N.; Millam J. M.; Klene M.; Knox J. E.; Cross J. B.; Bakken V.; Adamo C.; Jaramillo J.; Gomperts R.; Stratmann R. E.; Yazyev O.; Austin A. J.; Cammi R.; Pomelli C.; Ochterski J. W.; Martin R. L.; Morokuma K.; Zakrzewski V. G.; Voth G. A.; Salvador P.; Dannenberg J. J.; Dapprich S.; Daniels A. D.; Farkas Ö.; Foresman J. B.; Ortiz J. V.; Cioslowski J.; Fox D. J. Gaussian 09, Revision D.01, Gaussian, Inc, Wallingford CT, 2009.
- S2. Miehlich, B.; Savin, A.; Stoll, H.; Preuss, H. Results obtained with the correlation energy density functionals of Becke and Lee, Yang and Parr. *Chem. Phys. Lett.* 1989, 157, 200-206.
- S3. Axel, D.; Becke. Density-functional thermochemistry. II. The effect of the Perdew-Wang generalized-gradient correlation correction. *J. Chem. Phys.* 1992, 97, 9173-9177.
- S4. Cammi, J. R.; Corni, S.; Mennucci, B.; Tomasi, J. Electronic excitation energies of molecules in solution: state specific and linear response methods for nonequilibrium continuum solvation models. *Chem. Rev.* 2005, 105, 2999-3094.
- S5. Grimme S. Semiempirical GGA-type density functional constructed with a long-range dispersion correction. *J. Comput. Chem.* 2006, 27, 1787-1799.
- S6. Grimme S.; Antony J.; Ehrlich S.; Krieg H. A consistent and accurate ab initio parametrization of density functional dispersion correction (DFT-D) for the 94 elements H-Pu. *J. Chem. Phys.* 2010, 132, 154104-154108.

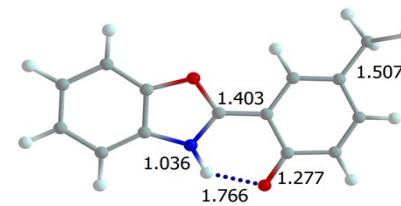




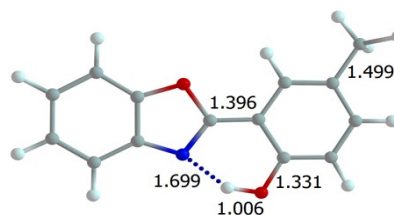
**syn-enol**  
**0**



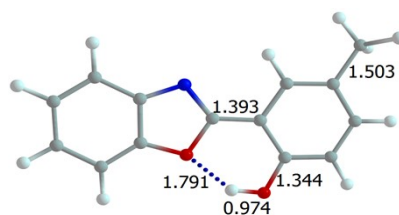
**anti-enol**  
**4.4**



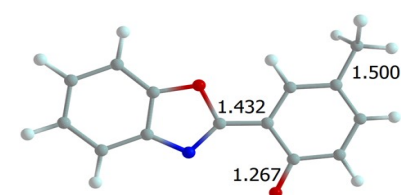
**keto**  
**9.2**



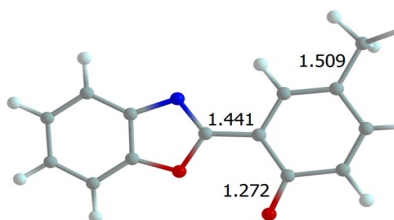
**syn-enol\***  
**75.4**



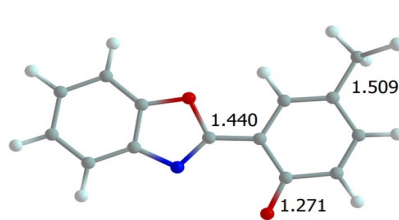
**anti-enol\***  
**81.2**



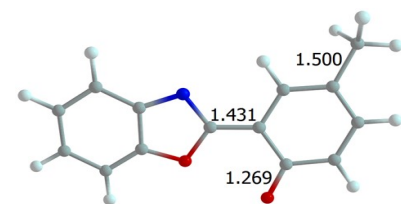
**anion**  
**297.9**



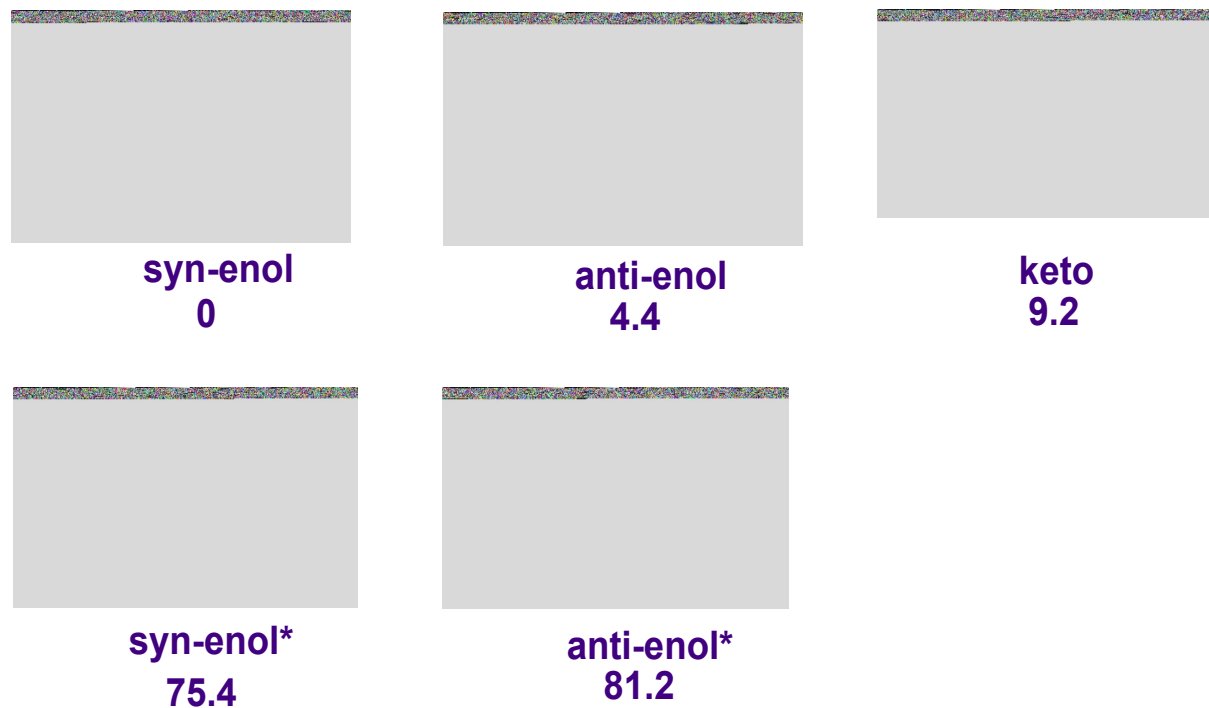
**anti-anion**  
**297.3**



**anion\***  
**359.6**



**anti-enol\***  
**359.1**



\* Minima of the corresponding first singlet excited states

**Figure S2.** Optimized structures and relative energy(in kcal/mol) of enol and keto HBO-pCH<sub>3</sub> as well as deprotonation forms in S<sub>0</sub> and S<sub>1</sub> calculated at the (TD-)B3LYP-D3(BJ)/6-311+G (d, p) level using PCM(solvent=methanol) model. Intra-molecular hydrogen bond distances are represented by dotted lines. Red: O; White: H; Blue: N; Gray: C.

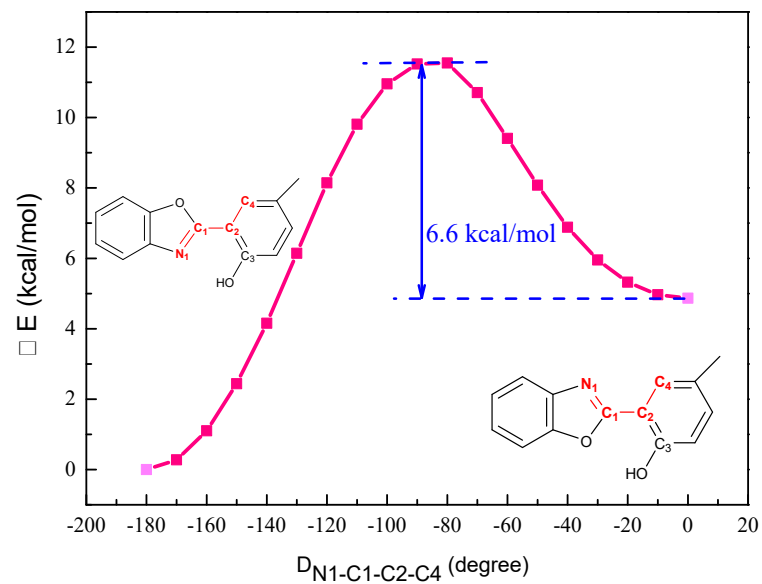
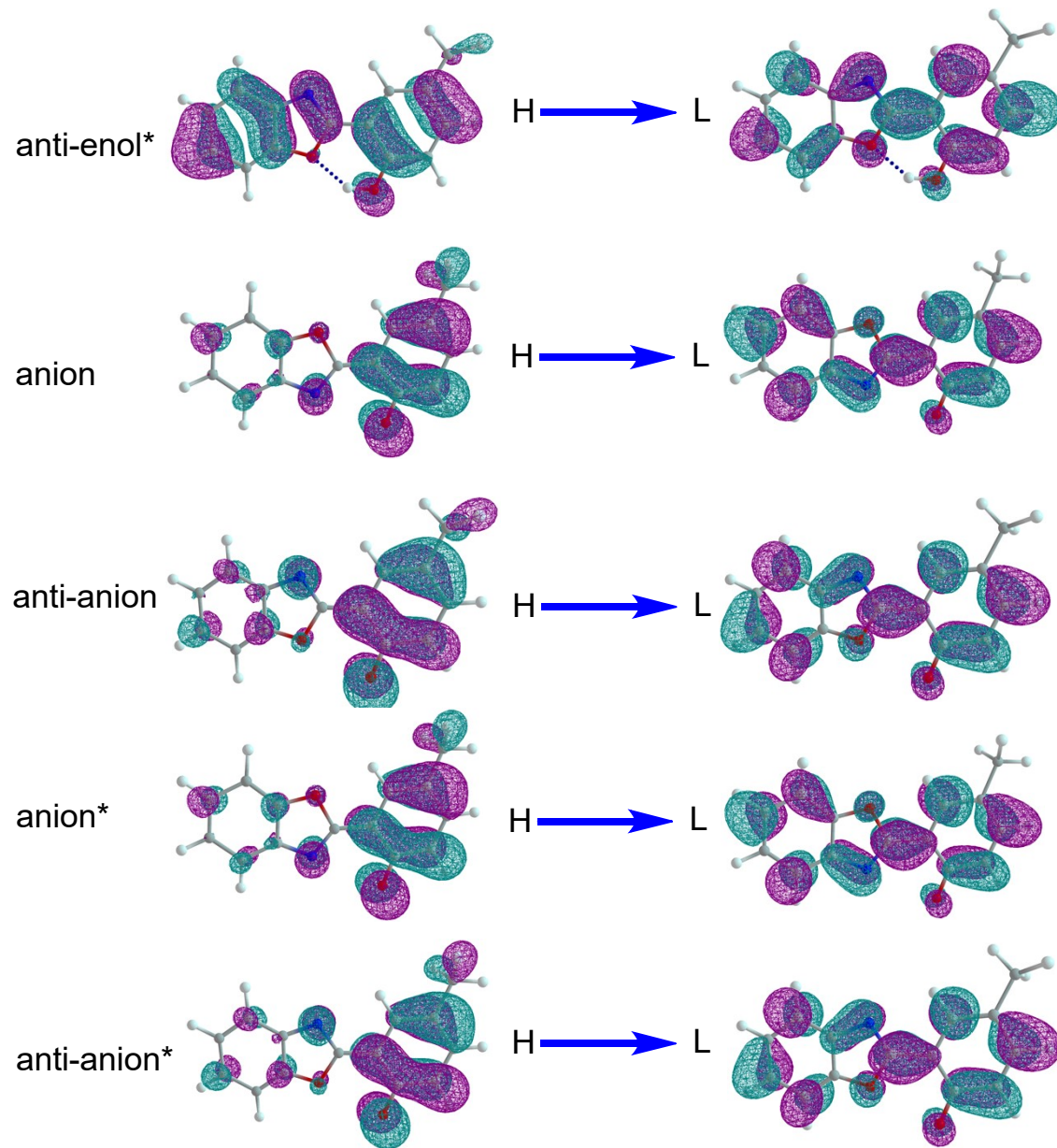


**Figure S3.** Potential energy curve of HBO-pCH<sub>3</sub> in the S<sub>0</sub> as a function of dehdal angle D<sub>N1-C1-C2-C4</sub> in methanol calculated at B3LYP-D3(BJ)/6-311+G (d, p) level using PCM(solvent=methanol) model.



\* Minima of the corresponding first singlet excited states

**Figure S4.** Optimized structures and relative energy(in kcal/mol) of enol and keto HBO-pCH<sub>3</sub> as well as deprotonation forms in S<sub>0</sub> and S<sub>1</sub> calculated at the (TD-)B3LYP-D3(BJ)/6-311+G (d, p) level using PCM(solvent=methanol) model. Intra-molecular hydrogen bond distances are represented by dotted lines. Red: O; Withe: H; Blue: N; Gray: C.





\* Minima of the corresponding first singlet excited states.

**Figure S5.** View of the frontier molecular orbitals (HOMO and LUMO) of HBO-pCH<sub>3</sub> under different condition calculated at (TD-)B3LYP-D3(BJ)/6-311+G (d, p) level using PCM(solvent=methanol) model.

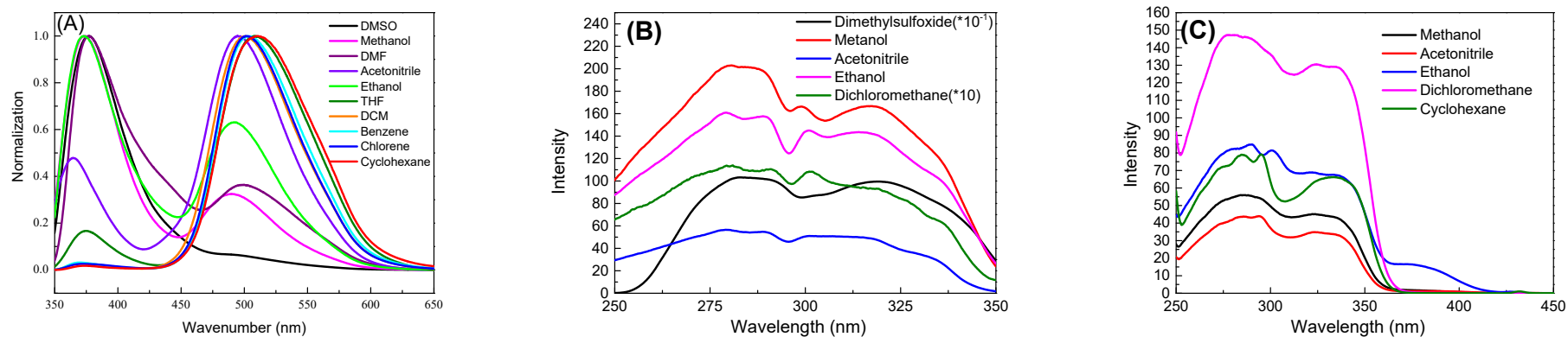


**Figure S6.** (A) Normalized emission spectra ( $\lambda_{ex}=330$  nm), (B) excitation spectra of HBO-pCH<sub>3</sub> in different solvents at ~375 nm, and (C) excitation spectra of HBO-pCH<sub>3</sub> in different solvents at ~495 nm. Condition: The concentration of HBO-pCH<sub>3</sub> was ~40  $\mu\text{mol/L}$  in solvents.

**Table S1.** Calculated emission wavelengths ( $\lambda_{em}$  (nm))/oscillator strengths(f) of TICTs (shown in Figure 9) at TD-B3LYP/6-311G(d,p) using PCM(solvent=methanol) model .

structure state	TICT-1	TICT-2	TICT-3	TICT-4
	$\lambda_{em}$ (nm)/f	$\lambda_{em}$ (nm)/f	$\lambda_{em}$ (nm)/f	$\lambda_{em}$ (nm)/f
S <sub>1</sub>	2036.8/0	2036.1/0	1424.9/0.0001	1426.3/0.0001
S <sub>2</sub>	649.5/0.0112	649.5/0.0112	540.1/0.1003	540.3/0.1004
S <sub>3</sub>	439.8/0	439.8/0	401.2/0.0002	401.3/0.0002

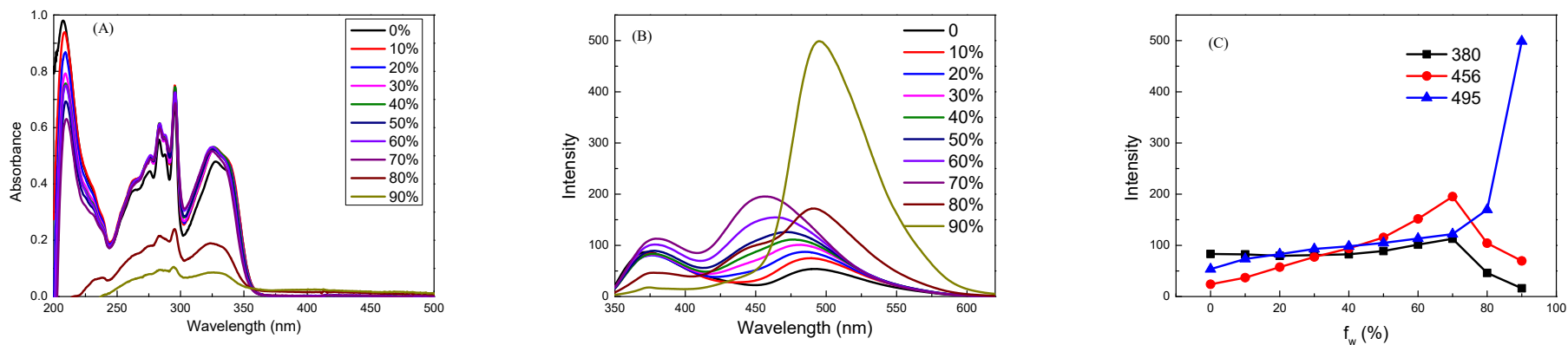


**Figure S7.** (A) Absorption spectra and (B) Emission spectra in water/ ethanol mixtures with different water fraction(  $f_w$ ). (C) Emission intensities at 380, 456, and 495 nm as functions of  $f_w$ . Conditions: Concentration of HBO-pCH<sub>3</sub> was  $\sim 40$   $\mu\text{mol/L}$ , excitation was at 330 nm.

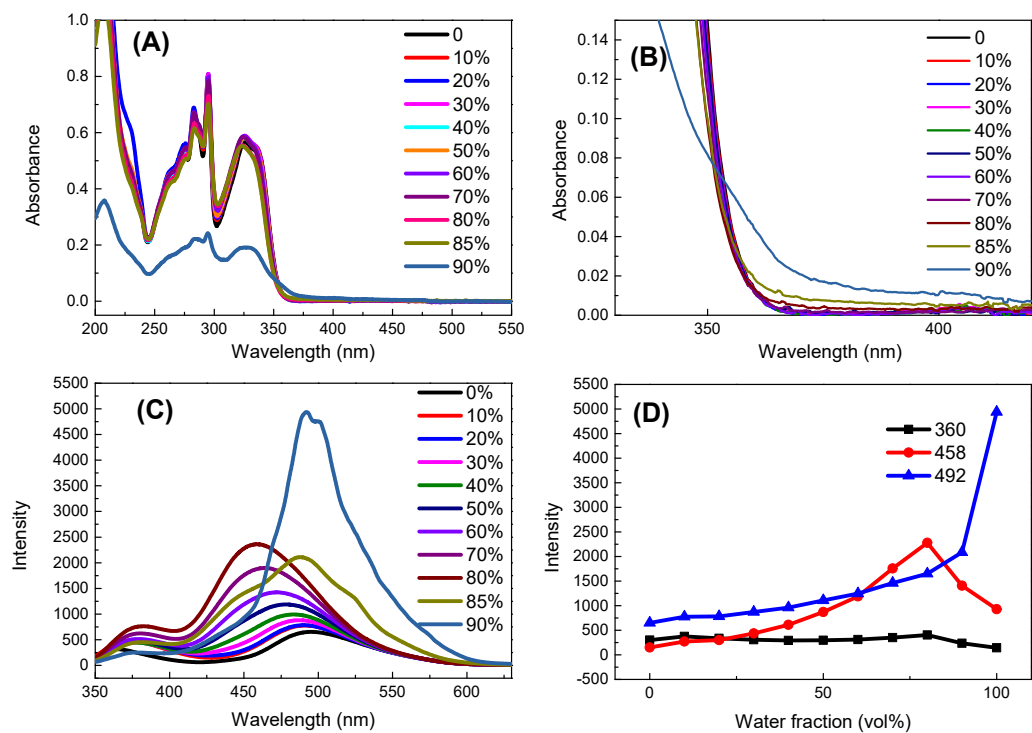


**Figure S8.** (A) Absorption spectra and (B) local enlargement of A); (C) emission spectra of HBO-pCH<sub>3</sub> in water/ acetonitrile mixtures with different water fraction ( $f_w$ ); (D) emissions at 360, 458, and 496 nm as functions of  $f_w$ . Conditions: Concentration of HBO-pCH<sub>3</sub> was  $\sim 40$   $\mu\text{mol/L}$ , excitation was at 330 nm.

